



# Soild-state decomposition mechanisms with conversion extent for ammonium perchlorate catalyzed with nanothermite particles

Abdelaziz Hamed<sup>1</sup> · Mohamed Gobara<sup>2</sup> · Mohamed Mokhtar<sup>1</sup> · Sherif Elbasuney<sup>1,2</sup>

Received: 2 November 2021 / Accepted: 17 July 2022 / Published online: 24 August 2022  
© The Author(s) 2022

## Abstract

Colloidal ferric oxide/aluminum nanothermite mixture was incorporated into ammonium perchlorate (AP). Nanothermite particles experienced an increase in AP decomposition enthalpy by 120% using DSC. Decomposition kinetic study was performed using integral isoconversional models including Kissinger and KAS models. Nanothermite particles offered decrease in AP activation energy by 55 and 44% using KAS and Kissinger models, respectively. AP nanocomposite is running through three decomposition steps according to extent of conversion: first-order decomposition with  $E_a = 41.08 \text{ kJ. mol}^{-1}$  ( $\alpha = 0: 0.25$ ), two-dimensional decomposition with  $E_a = 71.90 \text{ kJ. mol}^{-1}$  ( $\alpha = 0.25: 0.6$ ), and one-dimensional diffusion reaction with  $E_a = 97.10 \text{ kJ. mol}^{-1}$  ( $\alpha = 0.6: 0.9$ ).

**Keywords** Nanothermite · Catalyst · Thermal analysis · Decomposition kinetics

## Introduction

Ammonium perchlorate (AP) is the most frequently oxidizer for energetic systems [1]. AP can experience self-sustained combustion reaction [2, 3]. AP experience complex combustion process due to different chemical decomposition reactions that could take place [4]. Catalyst particles could play a significant role in AP thermal decomposition; metal oxides, i.e.,  $\text{Fe}_2\text{O}_3$ , can experience advanced catalytic effect [3, 5–8]. Ferric oxide nanoparticles can offer low activation energy and enhanced reaction propagation [9]. In the mean time, reactive metal fuels can offer enhanced AP performance. Nanoparticle dispersion to the molecular level can secure high interfacial surface area and reactivity [10]. Decomposition kinetics could be conducted via thermal analysis technique such as Differential Scanning Calorimetry (DSC) and Thermal Gravimetric Analysis (TGA). Isoconversional methods evaluate the relation between activation energy and the degree of conversion [11]. Nanothermite particles could have a great effect on decomposition parameters;

they could change the decomposition mechanism to metal fuel oxidation with high combustion temperature. AP encapsulation with nanothermite particles could offer superior catalytic activity with an increase in decomposition enthalpy. Kinetics of energetic material decomposition is essential to retrieve information of reaction mechanism, and shelf life estimation [12]. Kinetic parameters of decomposition reaction can be evaluated via Isoconversional method including Kissinger and KAS and models, respectively [13, 14]. This study reports on the development of nanothermite particles in continuous manner. Facile integration of colloidal nanothermite particles into AP matrix was accomplished via solvent/anti-solvent technique. Morphology of developed AP nanocomposite was investigated using Scanning Electron Microscopy SEM; particle dispersion was assessed with Electron Diffractive X-ray EDAX. Kinetic parameters of AP nanocomposite were investigated using KAS and Kissinger models in an attempt to investigate the mechanism of reaction propagation at different extent of conversion [15, 16]. To the best of the author's knowledge, this is the first time to integrate colloidal nanothermite particles into AP energetic matrix. This approach can eliminate nanoparticle drying and the re-dispersion of dry aggregates. The developed nanocomposite experienced superior decomposition kinetic parameters; as enhanced interfacial surface area could be accomplished [17].

✉ Sherif Elbasuney  
s.elbasuney@mtc.edu.eg; sherif\_basuney2000@yahoo.com

<sup>1</sup> School of Chemical Engineering, Military Technical College (MTC), Cairo, Egypt

<sup>2</sup> Nanotechnology Research Centre, Military Technical College (MTC), Cairo, Egypt

## Experimental work

### Materials

Ferric nitrate nonahydrate (Aldrich, 98%) was the employed metal salt precursor for synthesis of ferric oxide. Ammonium perchlorate (99%, Aldrich) was employed. The employed solvent and anti-solvent are acetone (99.5%, Aldrich) and Toluene 99%, (Aldrich), respectively.

### Synthesis of $\text{Fe}_2\text{O}_3$ NPs

Colloidal ferric oxide nanoparticles were synthesized via hydrothermal processing; further details about fabrication of ferric oxide particles can be found in the following references [18, 19]. Aluminum nanoplates of 100 nm were employed as reactive metal fuel.

### Integration of thermite particles into AP

Integration of thermite NPs into AP matrix was performed via solvent anti-solvent technique at room temperature, at which the solvent was acetone and the anti-solvent was toluene and diethyl ether solvent mixture and the mass added of NPs of aluminum was 5% and for ferric oxide was 1%. Ferric oxide NPs were harvested from their synthesis medium and re-dispersed in acetone using ultrasonic bath. Afterward aluminum NPs were dispersed in Ferric oxide colloid. AP particles were dissolved in nanothermite colloid; the anti-solvent was introduced. AP nanocomposite was precipitated, filtered, and dried (Fig. 1).

### Characterization of AP and AP nanocomposite

Morphology (shape and size) of virgin AP and AP nanocomposite was investigated using SEM ZEISS SEM EVO 10 MA. Nanoparticle dispersion through AP matrix was assessed using EDAX detector.

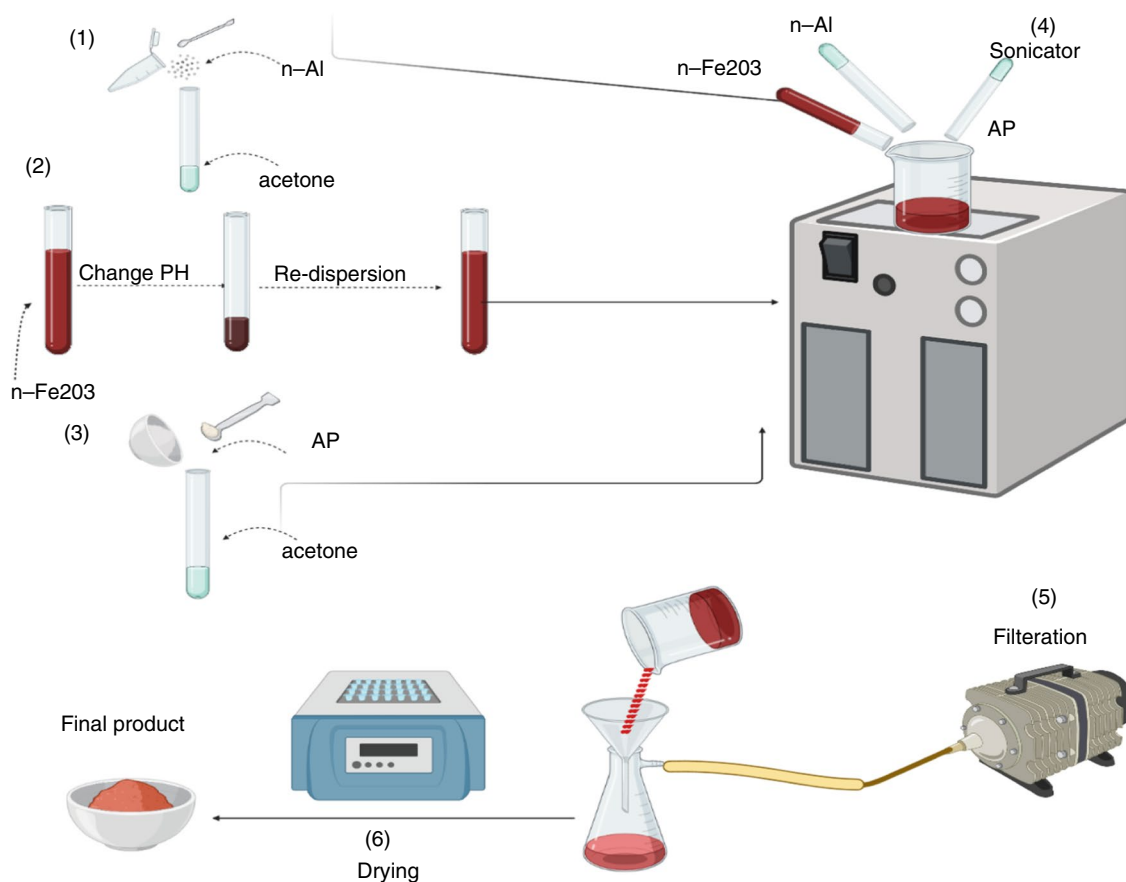


**Fig. 1** Development of AP nanocomposite via solvent anti-solvent technique

## Thermal behavior of AP nanocomposite

Thermal behavior of AP nanocomposite was conducted using DSC Q20 by TA instruments, USA. Tested sample (1 mg) was introduced to aluminum pan crucible and heated under nitrogen gas flow of (50 mL min<sup>-1</sup>) up to 500 °C at 10 °C min<sup>-1</sup>. Mass loss with temperature was further investigated using TGA Q500 by TA instruments, USA. Tested sample was heated at 10 °C min<sup>-1</sup> under N<sub>2</sub> flow of 50 mL min<sup>-1</sup>.

## Decomposition kinetics of AP nanocomposite

In this study, the impact of nanothermite particles on AP kinetic decomposition parameters were evaluated by using two methods. Integral isoconversional method was adopted using KAS (Eq. 1) [15].

$$\ln \left( \frac{\beta i}{T\alpha, i^{1.92}} \right) = \text{const} - 1.0008 \left( \frac{E\alpha}{RT\alpha} \right) \quad (1)$$

where  $\beta i$  is the heating rate,  $T$  is temperature at a known extent of conversion,  $R$  is the universal gas constant, and  $E\alpha$  is the apparent activation energy. Kissinger model (Eq. 2) was adopted for kinetic study. Further details on reaction propagation mechanism with extent of conversion can be found in the following reference [16].

$$\ln \left( \frac{\beta}{Tm, i^2} \right) = \ln \left( -\frac{AR}{E} f'(\alpha) \right) - \frac{E}{RTm, i} \quad (2)$$

where  $Tm$  is the maximum decomposition temperature,  $A$  is the pre-exponential factor, and  $f(\alpha)$  is the model of decomposition [20, 21].

## Results and discussions

### Characterization of AP nanocomposite

Morphology (size and shape) of virgin AP was visualized to developed AP nanocomposite using SEM. While virgin AP

demonstrated orthorhombic crystals with 150  $\mu\text{m}$  particle size (Fig. 2a), AP nanocomposite demonstrated fine crystals of 5  $\mu\text{m}$  particle size (Fig. 2b).

SEM micrographs demonstrated the successful integration of thermite particles into AP matrix. Figure 2a demonstrates the irregular crystal shape of AP of size range 50–200  $\mu\text{m}$ , and in Fig. 2b it is obvious the coagulation of AP particles, which could be attributed to the drying process, and the well dispersion of Al/Fe<sub>2</sub>O<sub>3</sub> nanoparticles on its surface. The reduction in particle size could be attributed to the facile re-crystallization via solvent anti-solvent technique. Elemental mapping using EDAX detector was conducted for virgin AP to assess the purity of virgin AP particles (Fig. 3).

Elemental analysis revealed the existence of the main AP elements. AP elemental composition was 12.2% for nitrogen, 0.5% for carbon, 56.6% for oxygen, and 30.7% for chlorine. AP nanocomposite elemental composition was 11.4% for nitrogen, 0.5% for carbon, 53.8% for oxygen, 0.9% for iron, 4.3% for Aluminum, and 29.1% for chlorine; this result is in accordance with the prepared composition samples. Elemental mapping of AP nanocomposite validated the uniform dispersion of nanothermites into the AP matrix (Fig. 4).

Uniform dispersion of nanothermite particles mainly of Al and Fe through the matrix was verified. Enhanced nanoparticle dispersion is vital for enhanced catalytic performance.

### Thermal behavior of AP nanocomposite

The impact of nanothermite particles on AP thermal behavior was assessed using DSC. Nanothermite particles boost AP decomposition enthalpy by 125%. While virgin AP demonstrated decomposition enthalpy of 918 J g<sup>-1</sup>; AP nanocomposite demonstrated decomposition enthalpy of 2068 J g<sup>-1</sup> (Fig. 5).

The enhanced decomposition enthalpy could be ascribed to the existence of aluminum as reactive metal fuel, and ferric oxide as catalyst particles [22]. Furthermore vigorous thermite reaction could be developed during AP

**Fig. 2** SEM micrographs of pure AP **a**, and AP nanocomposite **b**

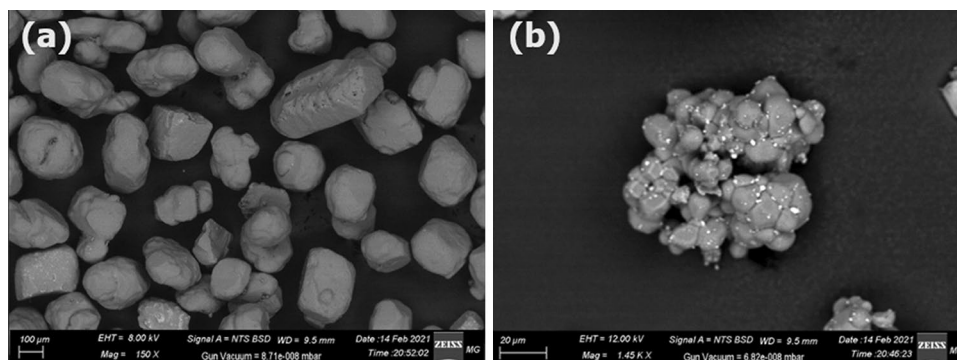


**Fig. 3** Elemental mapping of virgin AP using EDAX detector

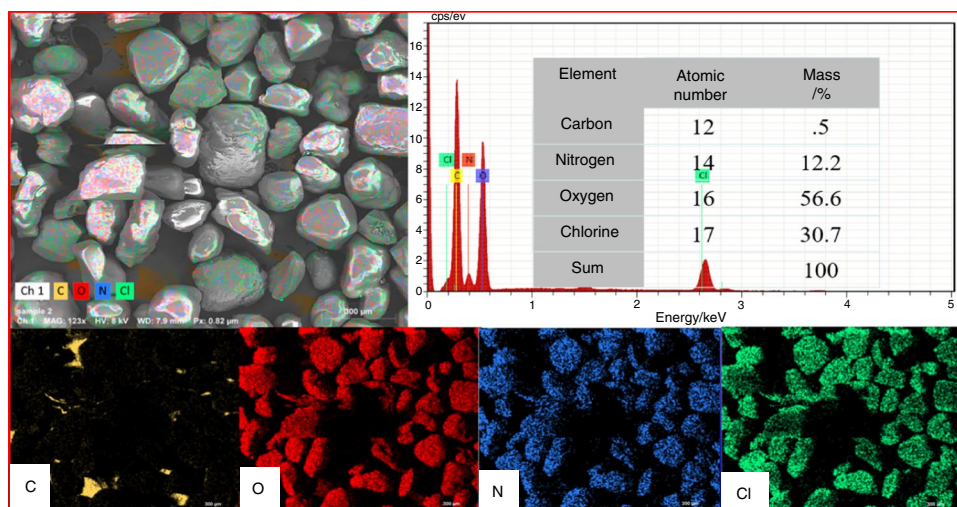
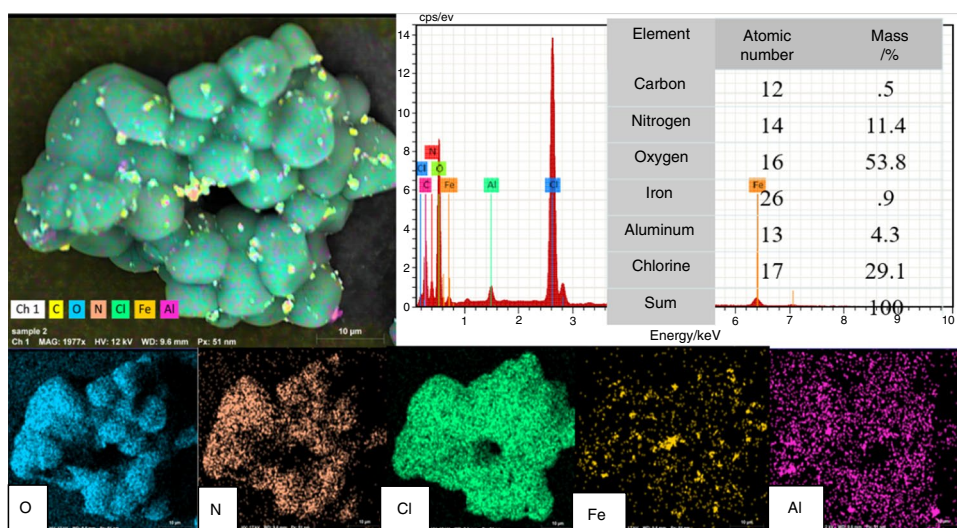


**Fig. 4** Elemental mapping of AP nanocomposite using EDAX detector



decomposition [23, 24]. The endothermic peak at 240 °C could be correlated to crystalline structure phase change from orthorhombic to cubic; at this point AP particles become unstable and degradation could start to take place [25]. The maximum decomposition temperature for the subsequent two main exothermic decomposition peaks has been reduced by 59 and 14 °C for high temperature decomposition (HTD) and low temperature decomposition (LTD), respectively.

### Catalytic decomposition of AP

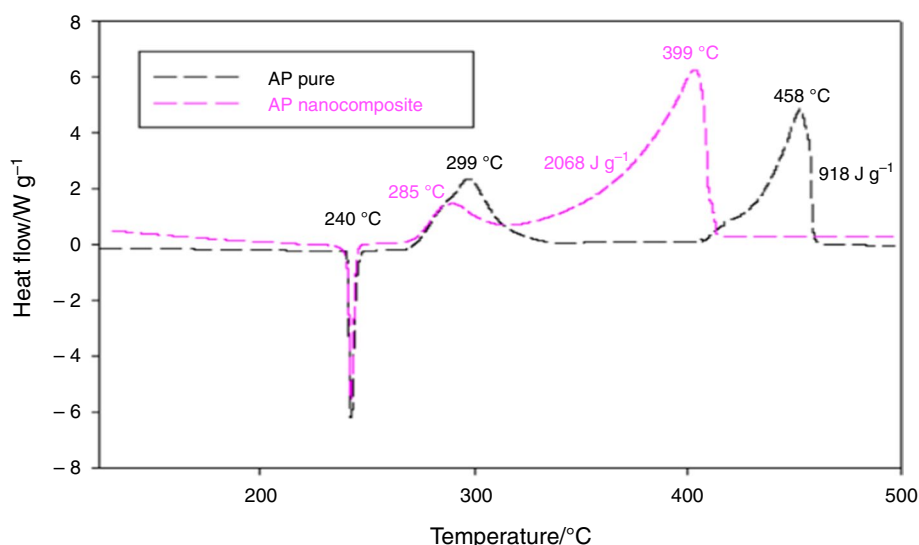
AP decomposition takes place through two main stages. Initial decomposition process at 299 °C with the evolution of ammonia and perchloric acid followed the final decomposition process at 458 °C with the release of final decomposition products [26–30]. The most acceptable mechanism of

AP decomposition is proton transfer mechanism (Fig. 6) [11] (Fig. 7).

Including ferric oxide nanocatalyst can absorb gas reactive molecules on its surface and boost the reaction rate and decomposition enthalpy [31]. Furthermore, the two exothermic decomposition peaks were shifted to a lower decomposition temperature and also the second decomposition peak started before the end of the first decomposition which confirms the rapid catalytic effect (Fig. 5). In addition, including n Al fuel increases the heat output. The proposed catalytic mechanism of AP decomposition after introducing nFe<sub>2</sub>O<sub>3</sub> and nAl additives depends mainly on the O<sub>2</sub><sup>-</sup> formation at the exterior surface of the catalyst. The negatively charged oxygen surface can act as proton trap for ammonium ion with the increase in the rate of NH<sub>3</sub> production [29, 32].



**Fig. 5** DSC curve of virgin AP to AP nanocomposite



AP decomposition with result in the evolution free oxygen rich; this oxygen would react with reactive nAl with the increase in total heat release [33].

### Decomposition kinetics of AP nanocomposite

Activation energy and kinetic parameters were evaluated using KAS and the Kissinger models. AP nanothermite was heated at three different heating rate of 3, 5, 7 °C min<sup>-1</sup> under N<sub>2</sub> flow of (50 mL min<sup>-1</sup>) up to 500 °C using DSC (Fig. 8).

The first and second exothermic decomposition peaks shifted to high value with increase in heating rate [34]. Furthermore; the extent of conversion (fraction reacted) with temperature curve was plotted (Fig. 9).

The solid-state decomposition mechanism of AP nanocomposite could be predicted by monitoring the degree of conversion at different temperature values. These parameters can be interpreted via best fitting to different decomposition reaction mechanism models. Therefore decomposition parameters and decomposition mechanism could be interpreted.

### Kinetic study using KAS model

The activation energy at different extent of fraction reacted was calculated to retrieve the apparent activation energy. Table 1 indicates the kinetic parameters calculated by the integral isoconversional KAS model.

Nanothermite particles offered decrease in AP activation energy by 55%, Whereas virgin AP demonstrated an activation energy of 157.9 kJ.mol<sup>-1</sup>; AP nanocomposite demonstrated an activation energy of 71 kJ.mol<sup>-1</sup> [35].

This finding confirmed the advanced catalytic effect of the nanothermite additives on the AP powder. The plot of activation energy at different conversion extent is demonstrated in Fig. 10.

It is obvious that the fluctuated activation energy range at different extent of conversion indicated that AP nanocomposite decomposition encompass three main stages according to extent of fraction reacted ( $\alpha$ ). AP decomposition could be performed in different steps of reactions due to different interactions possibility of the produced different gas phase constituents in the reaction media. In addition, added NPs to AP make the mechanism of the reaction is more complicated.

### Kinetic study using the Kissinger model

The apparent activation energy was calculated by using the Kissinger model via the slope of the straight line  $\ln\left(\frac{\beta}{T_{m,i}^2}\right)$  versus  $\left(\frac{1}{T_{m,i}}\right)$  (Fig. 11).

Again nanothermite particles experienced decrease in AP activation energy by 44%. While the apparent activation energy of virgin was reported to be 121.5 kJ.mol<sup>-1</sup>, the apparent activation energy of the synthesized AP nanothermite was 68.5 kJ.mol<sup>-1</sup> [28].

It is obvious that nanothermite particles offered a dramatic change in AP activation energy. Thermal decomposition AP is complicated process; decomposition mechanism could vary with extent of fraction reacted. To sum up, Kissinger model is recommended for nanothermite particles AP to determine accurately its activation energy because the results of the three different heating rates had the same extent of conversion at 80%.

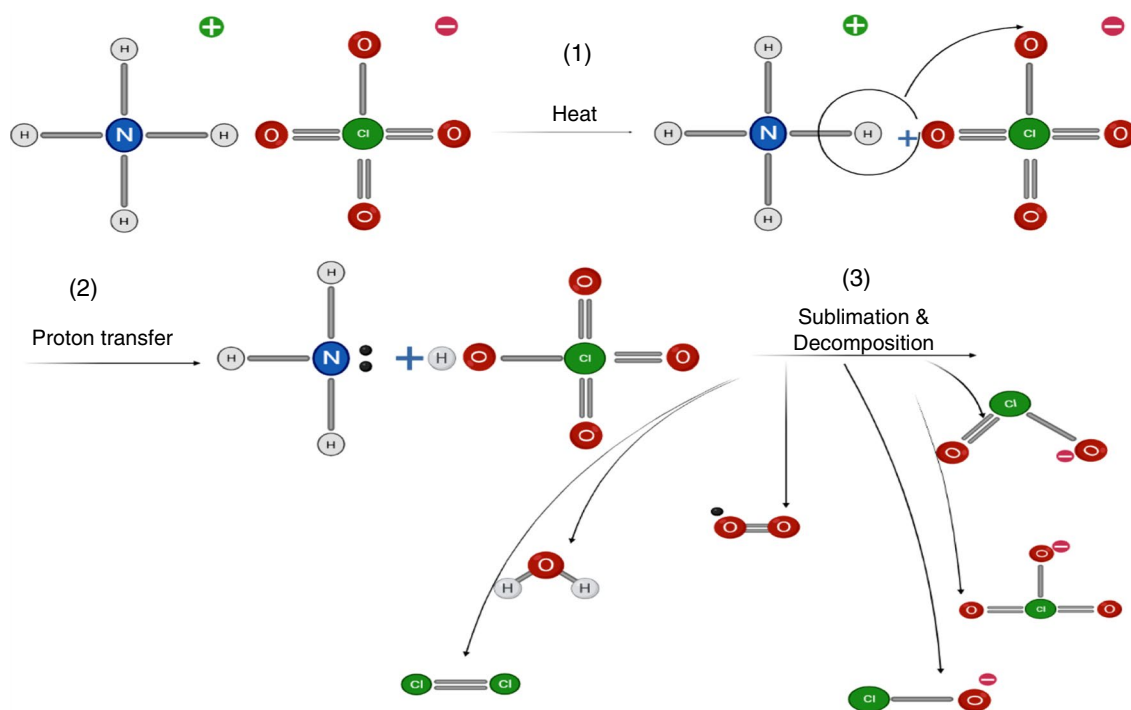


Fig. 6 Schematic for AP decomposition mechanism

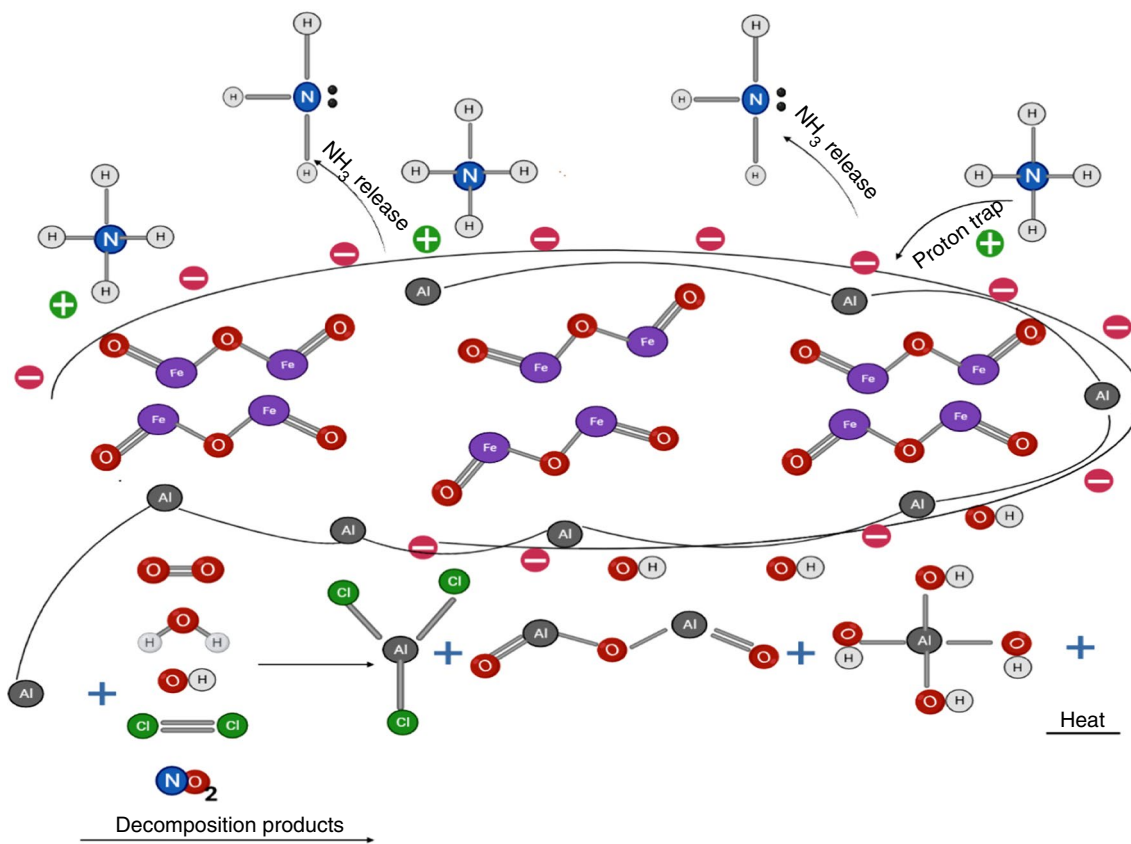
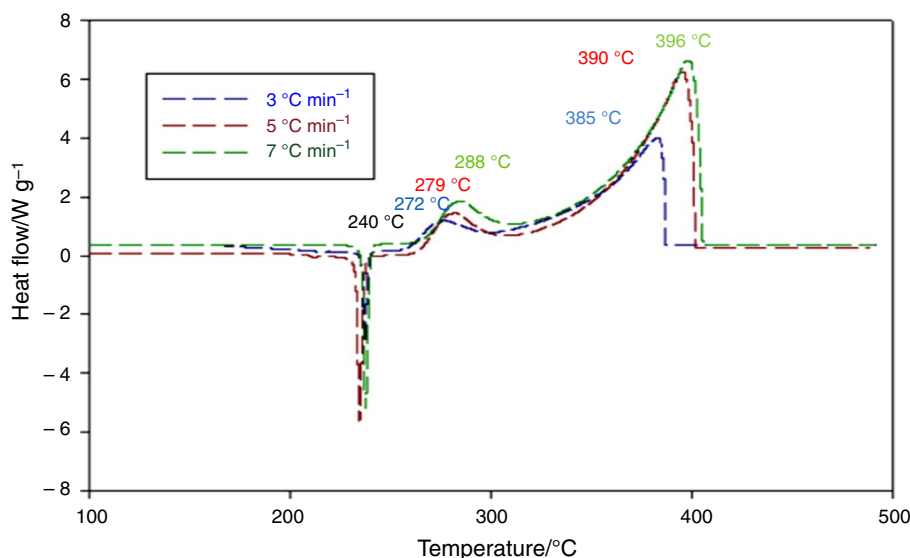
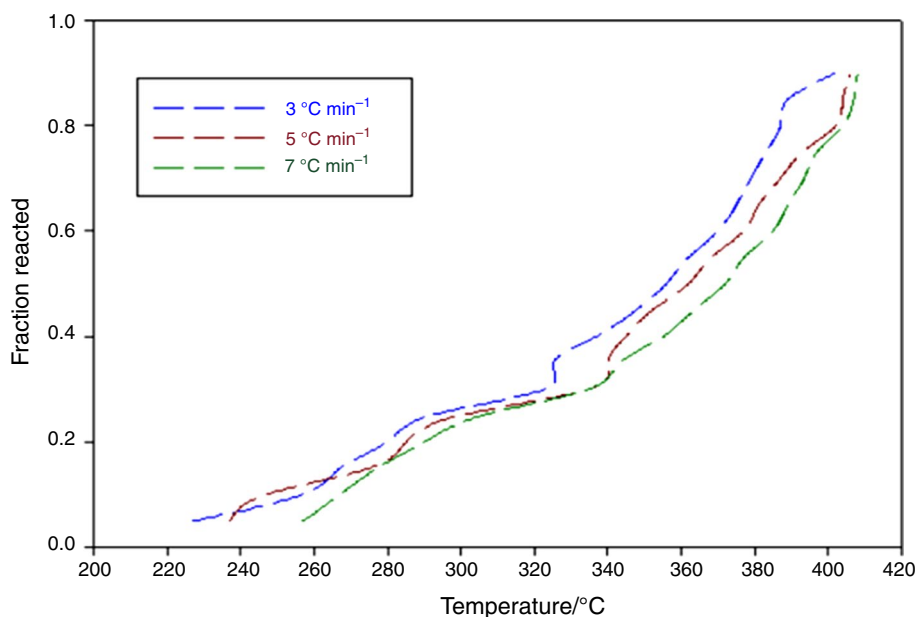


Fig. 7 Proposed mechanism for catalyzed AP decomposition

**Fig. 8** DSC curve of different heating rates for AP nanocomposite



**Fig. 9** Fraction reacted with temperature at different heating rates



**Decomposition model of AP nanocomposite**

Decomposition mechanism can be predicted via the relation of different kinetic decomposition parameters such as fraction reacted, rate of change of fraction reacted, and the temperature [36]. The mechanism of decomposition can be evaluated via the plot of fraction reacted with temperature (Fig. 12).

The mechanism of decomposition of AP nanocomposite started with first-order decomposition and ended with the diffusion decomposition mechanism. The previous result indicated that AP nanocomposite decomposes in steps. However; the mechanisms are shifted to be decelerating. The catalytic effect of nanothermite on AP powder was confirmed by the decreasing in the values of the apparent activation energy in comparison with the pure one, and

**Table 1** Kinetic parameters of AP nanocomposite using KAS model

$\alpha$	$E_a/\text{kJ}\cdot\text{mol}^{-1}$	$\text{Log } A/\text{s}^{-1}$	$\text{K/s}^{-1}$	$R$
0.05	050.50	02.30	2.10 E-3	0.895
0.10	044.90	03.30	2.30 E-3	0.924
0.15	033.00	03.72	3.80	0.864
0.20	037.00	03.84	3.90	0.805
0.25	040.00	03.55	3.95	0.936
0.30	055.90	04.35	5.30	0.978
0.35	070.00	04.69	6.11	0.949
0.40	071.00	05.77	6.47	0.919
0.45	073.00	06.68	10.10	0.967
0.50	073.50	06.22	11.15	0.939
0.55	075.00	07.64	17.80	0.957
0.60	085.00	08.57	40.99	0.927
0.65	090.00	09.37	250.20	0.962
0.70	103.00	08.88	254.40	0.948
0.75	105.00	09.72	281.00	0.961
0.80	107.00	10.51	287.90	0.993
0.85	098.00	10.38	300.00	0.941
0.90	080.00	10.69	305.00	0.848
Mean	071.00	06.67	–	–

also the mechanism was shifted to be decelerating other than autocatalytic [37]. Furthermore the relation of conversion extent and the rate of change of extent of conversion is represented in Fig. 13.

It is obvious that the mechanism of decomposition is running in three steps as follows:

First step is first-order decomposition reaction with  $E_a = 41.08 \text{ kJ}\cdot\text{mol}^{-1}$  for ( $\alpha = 0:0.25$ ).

Second step is two-dimensional decomposition reaction with  $E_a = 71.90 \text{ kJ}\cdot\text{mol}^{-1}$  for ( $\alpha = 0.25:0.6$ ).

Third step is one-dimensional diffusion reaction with  $E_a = 97.10 \text{ kJ}\cdot\text{mol}^{-1}$  for ( $\alpha = 0.6:0.9$ ).

## Conclusions

Colloidal nanoferric oxide was fabricated by using hydrothermal synthesis. Nanothermite  $\text{Al}/\text{Fe}_2\text{O}_3$  particles were integrated successfully into AP matrix via solvent anti/solvent technique. Shape, size, and elemental mapping of AP/AP nanothermite were conducted using SEM instrument and revealed good dispersion of nanothermite into AP matrix. Nanothermite particles experienced an increase in AP decomposition enthalpy by 125% using DSC. Decomposition kinetic study of AP nanocomposite was performed using integral isoconversional models including Kissinger and KAS models. AP nanocomposite is running through three decomposition steps according to extent of conversion: first-order decomposition mechanism with  $E_a = 41.08 \text{ kJ}\cdot\text{mol}^{-1}$  ( $\alpha = 0: 0.25$ ), two-dimensional decomposition reaction with  $E_a = 71.90 \text{ kJ}\cdot\text{mol}^{-1}$  ( $\alpha = 0.25: 0.6$ ), and one-dimensional diffusion reaction with  $E_a = 97.10 \text{ kJ}\cdot\text{mol}^{-1}$  ( $\alpha = 0.6:0.9$ ). Integration of nanothermites catalyzes the decomposition reaction of ammonium perchlorate.

**Fig. 10** Activation energy of AP nanocomposite at different fraction reacted using KAS model

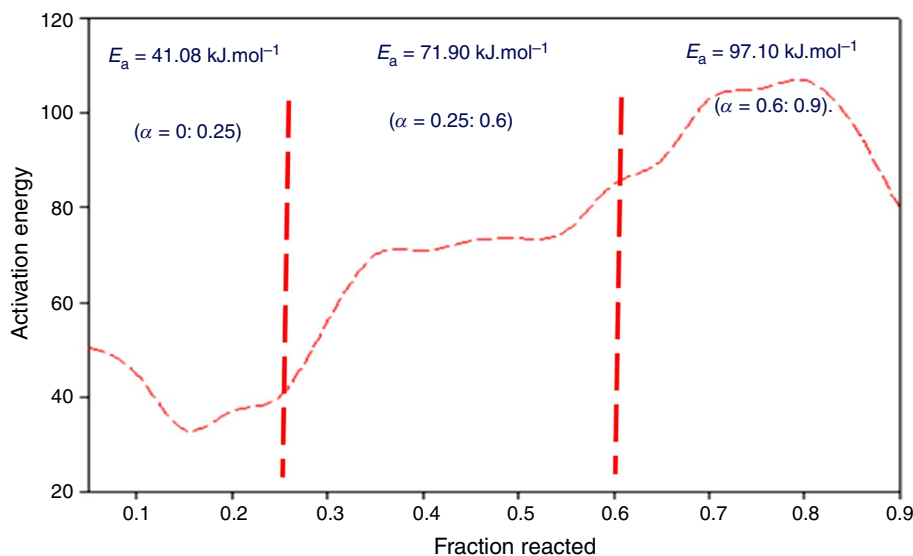


**Fig. 11** Activation energy of AP nanocomposite using Kissinger model

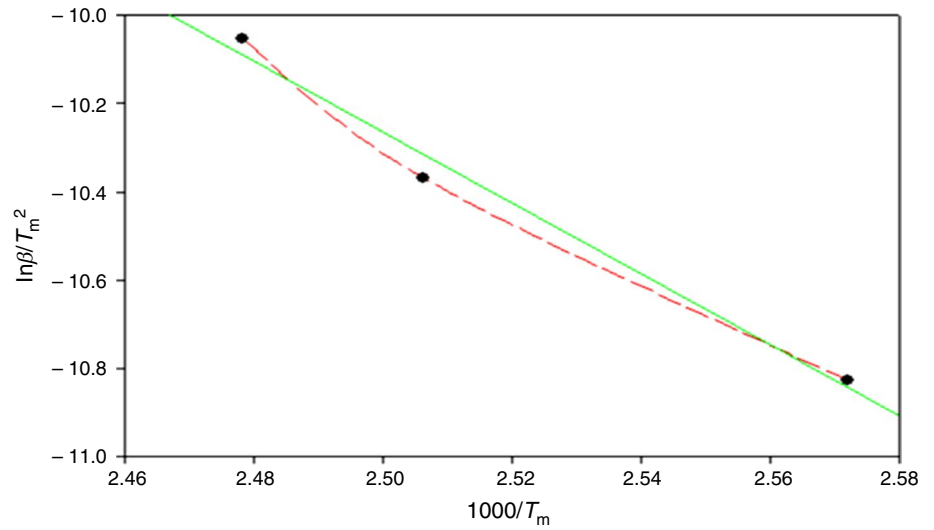


**Fig. 12** Plot of fraction reacted and temperature for heterogeneous decomposition reaction of AP nanocomposite

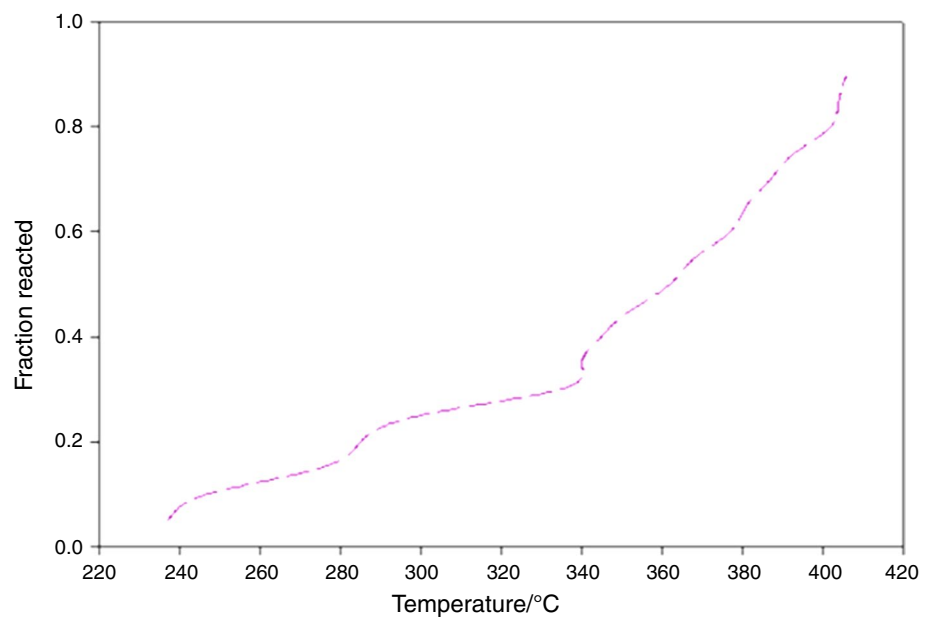
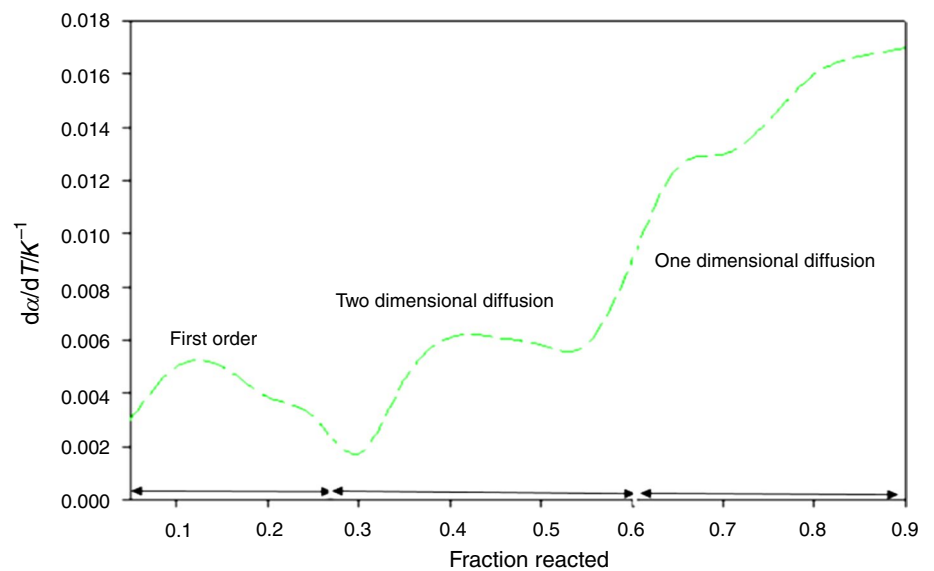


**Fig. 13** Plot of fraction reacted ( $\alpha$ ) and ( $d\alpha/dT$ ) for heterogeneous decomposition reaction of AP nanocomposite



**Funding** Open access funding provided by The Science, Technology & Innovation Funding Authority (STDF) in cooperation with The Egyptian Knowledge Bank (EKB).

**Open Access** This article is licensed under a Creative Commons Attribution 4.0 International License, which permits use, sharing, adaptation, distribution and reproduction in any medium or format, as long as you give appropriate credit to the original author(s) and the source, provide a link to the Creative Commons licence, and indicate if changes were made. The images or other third party material in this article are included in the article's Creative Commons licence, unless indicated otherwise in a credit line to the material. If material is not included in the article's Creative Commons licence and your intended use is not permitted by statutory regulation or exceeds the permitted use, you will need to obtain permission directly from the copyright holder. To view a copy of this licence, visit <http://creativecommons.org/licenses/by/4.0/>.

## References

- Rajić M, Sućeska M. Study of thermal decomposition kinetics of low-temperature reaction of ammonium perchlorate by isothermal TG. *J Therm Anal Calorim.* 2000;63(2):375–86.
- Beckstead MW, et al. Modeling of combustion and ignition of solid-propellant ingredients. *Prog Energy Combust Sci.* 2007;33(6):497–551.
- Chaturvedi S, Dave PN. Nano-metal oxide: potential catalyst on thermal decomposition of ammonium perchlorate. *J Exp Nanosci.* 2012;7(2):205–31.
- Brill TB, Ren W-Z, Yang V. Solid propellant chemistry, combustion, and motor interior ballistics. California: American Institute of Aeronautics and Astronautics; 2000.
- Zhi J, et al. Thermal behavior of ammonium perchlorate and metal powders of different grades. *J Therm Anal Calorim.* 2006;85(2):315–20.
- Nunes Almeida LE, et al. Thermal decomposition kinetics studies of ammonium perchlorate-HTPB/Al/AP solid propellants formulated with iron oxide burning rate catalyst in Nano and Micro scale, in *49th AIAA/ASME/SAE/ASEE Joint Propulsion Conference.* 2013; p. 4088.
- Singh G, et al. Effect of mixed ternary transition metal ferrite nanocrystallites on thermal decomposition of ammonium perchlorate. *Thermochim Acta.* 2008;477(1–2):42–7.
- Peiris, SM, Pangilinan G, and Russell T, Structural properties of ammonium perchlorate compressed to 5.6 GPa. *J Phys Chem A,* 2000; **104**(47) p.11188–11193.
- Fujimura K, Miyake A. Effect of the particle size of ferric oxide on the thermal decomposition of AP-HTPB composite propellant. *Sci Technol Energy Mater.* 2008;69:149–54.
- Liu P, et al. Preparation and catalytic activity of Fe<sub>2</sub>O<sub>3</sub>/CNT to thermal decomposition of ammonium perchlorate. In: *Advanced Materials Research.* 2012. Trans Tech Publ, Switzerland.
- Yan Q-L, et al. Catalytic effects of nano additives on decomposition and combustion of RDX-, HMX-, and AP-based energetic compositions. *Prog Energy Combust Sci.* 2016;57:75–136.
- Vyazovkin S, et al. ICTAC kinetics committee recommendations for performing kinetic computations on thermal analysis data. *Thermochim Acta.* 2011;520(1–2):1–19.
- Vyazovkin S, Sbirrazzuoli N. Isoconversional kinetic analysis of thermally stimulated processes in polymers. *Macromol Rapid Commun.* 2006;27(18):1515–32.
- Vyazovkin S, Wight CA. Model-free and model-fitting approaches to kinetic analysis of isothermal and nonisothermal data. *Thermochim Acta.* 1999;340:53–68.
- Akahira T, Sunose T. Method of determining activation deterioration constant of electrical insulating materials. *Res Rep Chiba Inst Technol Sci Technol.* 1971;1971(16):22–31.
- Kissinger HE. Reaction kinetics in differential thermal analysis. *Anal Chem.* 1957;29(11):1702–6.
- Khasainov B, et al. Comparison of performance of fast-reacting nanothermites and primary explosives. *Propell Explos Pyrotech.* 2017;42(7):754–72.
- Elbasuney S, et al. Ferric oxide colloid: novel nanocatalyst for heterocyclic nitramines. *J Mater Sci: Mater Electron.* 2021;32(4):4185–95.
- Elbasuney S, et al. Super-thermite (Al/Fe<sub>2</sub>O<sub>3</sub>) fluorocarbon nanocomposite with stimulated infrared thermal signature via extended primary combustion zones for effective countermeasures of infrared seekers. *J Inorg Organomet Polym Mater.* 2018;28(6):2231–40.
- Atkins P, and de Paula J, *Atkins physical chemistry* (9th Czech edition). VŠCHT, Praha, 2013; p. 705–732.
- Brown ME. *Introduction to thermal analysis: techniques and applications*, vol. 1. Netherlands: Springer; 2001.
- Yetter RA, Risha GA, Son SF. Metal particle combustion and nanotechnology. *Proc Combust Inst.* 2009;32(2):1819–38.
- Elbasuney S, et al. Synergistic catalytic effect of thermite nanoparticles on HMX thermal decomposition. *J Inorganic Organomet Polym Mater,* 2021; p. 1–13.
- Elbasuney S, et al. The significant impact colloidal nanothermite particles (Fe<sub>2</sub>O<sub>3</sub>/Al) on HMX kinetic decomposition. *J Energetic Mater,* 2021; p. 1–16.
- Wang H, et al. Assembly and encapsulation of aluminum NP's within AP/NC matrix and their reactive properties. *Combust Flame.* 2017;180:175–83.
- Singh G, et al. Preparation, characterization and catalytic activity of transition metal oxide nanocrystals. In: *Journal of Scientific Conference Proceedings.* American Scientific Publishers, California (2009)
- Xu H, Wang X, Zhang L. Selective preparation of nanorods and micro-octahedrons of Fe<sub>2</sub>O<sub>3</sub> and their catalytic performances for thermal decomposition of ammonium perchlorate. *Powder Technol.* 2008;185(2):176–80.
- Joshi S, Patil PR, Krishnamurthy V. Thermal decomposition of ammonium perchlorate in the presence of nanosized Ferric Oxide. *Def Sci J.* 2008;58(6):721–7.
- Li L, et al. Nature of catalytic activities of CoO nanocrystals in thermal decomposition of ammonium perchlorate. *Inorg Chem.* 2008;47(19):8839–46.
- Zhao S, Ma D, Jin W. Preparation of Co Fe<sub>2</sub>O<sub>4</sub> nanocrystallites by solvothermal process and its catalytic activity on the thermal decomposition of ammonium perchlorate. *J Nanomater.* 2010;2010:28.
- Elbasuney S. et al. The impact of metastable intermolecular nanocomposite particles on kinetic decomposition of heterocyclic using advanced solid-phase decomposition models. *J Inorganic Organomet Nitramines Polym Mater,* 2021; p. 1–12.
- Chen L, Li L, Li G. Synthesis of CuO nanorods and their catalytic activity in the thermal decomposition of ammonium perchlorate. *J Alloy Compd.* 2008;464(1–2):532–6.
- Zongxue Y, et al. DSC/TG-MS study on in situ catalytic thermal decomposition of ammonium perchlorate over CoC<sub>2</sub>O<sub>4</sub>. *Chin J Catal.* 2009;30(1):19–23.
- Yan Q-L, et al. Thermal behavior and decomposition kinetics of Formex-bonded explosives containing different cyclic nitramines. *J Therm Anal Calorim.* 2013;111(2):1419–30.

35. Li X, Yang R, and Li X, The functional additveis CNTs, conference paper in Propellants Explos. Proeed Xi'an Mod Chem Res Inst, 2004; p. 228–231.
36. Khawam A, Flanagan DR. Solid-state kinetic models: basics and mathematical fundamentals. J Phys Chem B. 2006;110(35):17315–28.
37. Vyazovkin S, Wight CA. Kinetics of thermal decomposition of cubic ammonium perchlorate. Chem Mater. 1999;11(11):3386–93.

**Publisher's Note** Springer Nature remains neutral with regard to jurisdictional claims in published maps and institutional affiliations.